Advanced Robotics, Vol. 20, No. 7, pp. 763–781 (2006)

Also available online - www.vsppub.com

Full paper

Kinematic, singularity and stiffness analysis of the hydraulic shoulder: a 3-d.o.f. redundant parallel manipulator

H. SADJADIAN and H. D. TAGHIRAD *

Advanced Robotics and Automated Systems Research Group, Electrical Engineering Department, K. N. Toosi University of Technology, PO Box 16315-1355, Tehran, Iran

Received 24 May 2005; accepted 5 September 2005

Abstract—In this paper, kinematic modeling and singularity and stiffness analysis of a 3-d.o.f. redundant parallel manipulator have been elaborated in detail. It is known that, contrary to series manipulators, the forward kinematic map of parallel manipulators involves highly coupled non-linear equations, whose closed-form solution derivation is a real challenge. This issue is of great importance noting that the forward kinematics solution is a key element in closed-loop position control of parallel manipulators. Using the idea of inherent kinematic chains formed in parallel manipulators, both inverse and forward kinematics of the redundant parallel manipulator are fully developed, and a closed-form solution for the forward kinematic map of the parallel manipulator is derived. The closed-form solution is also obtained in detail for the Jacobian of the mechanism and singularity analysis of the manipulator is performed based on the computed Jacobian. Finally, as the first step to develop a control topology based on the overall stiffness property of the manipulator, the stiffness mapping of the manipulator is derived and its configuration dependence is analyzed. It is observed that the actuator redundancy in the mechanism is the major element to improve the Cartesian stiffness and, hence, the dexterity of the hydraulic shoulder. Moreover, loosing one limb actuation reduces the stiffness of the manipulator significantly.

Keywords: Parallel manipulator; kinematic modeling; forward kinematics; Jacobian analysis; stiffness mapping.

1. INTRODUCTION

Over the last two decades parallel manipulators have been among the most important research topics in the field of robotics. A parallel manipulator typically consists of a moving platform that is connected to a fixed base by several limbs. The number of limbs is at least equal to the number of degrees of freedom (d.o.f.) of the mov-

*To whom correspondence should be addressed. E-mail: taghirad@kntu.ac.ir

ing platform so that no more than one actuator drives each limb and all actuators can be mounted on or near the fixed base. These robots are now used in real-life applications such as force-sensing robots, fine-positioning devices and medical manipulators [1, 2]. In the literature, mostly 6-d.o.f. parallel mechanisms based on the Stewart–Gough platform are analyzed [3]. However, parallel manipulators with 3 d.o.f. have been also implemented for applications where 6 d.o.f. are not required, such as high-speed machine tools. Recently, 3-d.o.f. parallel manipulators with more than three limbs have been among the investigated mechanisms, in which the additional limb is introduced to avoid singular configurations at the cost of increased mechanical complexity [4]. Complete kinematic modeling and Jacobian analysis of such mechanisms have not received much attention so far, and is still regarded as an interesting problem in parallel robotics research.

It is known that unlike serial manipulators, inverse position kinematics for parallel robots is usually simple and straightforward. In most cases joint variables may be computed independently using the given pose of the moving platform. The solution to this problem in most cases is uniquely determined. However, forward kinematics of parallel manipulators is generally very complicated. Its solution usually involves systems of non-linear equations, which are highly coupled, and in general have no closed-form and unique solution. Different approaches are provided in the literature to solve this problem either in general or in special cases. There are also several cases in which the solution to this problem is obtained for a special or novel architecture [5–9]. Two such special 3-d.o.f. constrained mechanisms have been studied in Refs [10, 11], where kinematics, Jacobian and dynamics have been considered for such manipulators. Joshi and Tsai [4] performed a detailed comparison between a 3-UPU and the so-called Tricept manipulator regarding the kinematic, workspace and stiffness properties of the mechanisms. In general, different solutions to the forward kinematics problem of parallel manipulators can be found using numerical or analytical approaches, or a closed-form solution for special architectures [12, 13].

In this paper, complete kinematic modeling for a 3-d.o.f. actuator redundant hydraulic parallel manipulator has been performed and a closed-form forward kinematics solution is obtained. The mechanism is designed by Hayward [14–16], borrowing design ideas from biological manipulators, particularly the biological shoulder. The interesting features of this mechanism and its similarity to the human shoulder have made its design unique, which can serve as a basis for a good experimental setup for parallel robotics research. This design is different from the usual Tricepts-type parallel manipulators, since it incorporates redundancy in manipulator actuation. In a former study by the authors, different numerical approaches have been used to solve the forward kinematic map of this manipulator [17]. The numerical approaches are an alternative to estimate the forward kinematic solution, in case such solutions cannot be obtained in closed form. In this paper, however, the idea of kinematic chains developed for parallel manipulators structures [10, 11] is applied for the manipulator and it is observed that the closed-form

kinematic solution for this manipulator can be obtained in detail in a systematic manner. Using the closed-form forward kinematic map of the manipulator, a kinematic analysis for the manipulator is performed on the Jacobians, singularities and stiffness mapping. The Jacobian matrix of the manipulator is derived through a complete velocity analysis of the mechanism and a thorough singularity analysis is performed using the configuration-dependent Jacobian. Through this analysis the original claim of the mechanism designer, that the mechanism is singularity free, is verified. Finally, the stiffness analysis of the mechanism has been elaborated, resulting in the stiffness matrix, and the minimum and maximum stiffness mappings of the hydraulic shoulder. This analysis is the base of proposing control topologies on the mechanism based on the stiffness mappings.

2. MECHANISM DESCRIPTION

A schematic of the mechanism currently under experimental studies in the ARAS Robotics Laboratory is shown in Fig. 1. The mobile platform is constrained to spherical motions. Four high-performance hydraulic piston actuators are used to give 3 d.o.f. in the mobile platform.

Each actuator includes a position sensor of the LVDT type and an embedded Hall effect force sensor. The four limbs share an identical kinematic structure. A passive limb connects the fixed base to the moving platform by a spherical joint, which suppresses the pure translations of the moving platform. Simple elements like spherical and universal joints are used in the structure. From the structural point of view, the shoulder mechanism, which from now on we call 'the hydraulic shoulder', falls into an important class of robotic mechanisms called parallel robots.

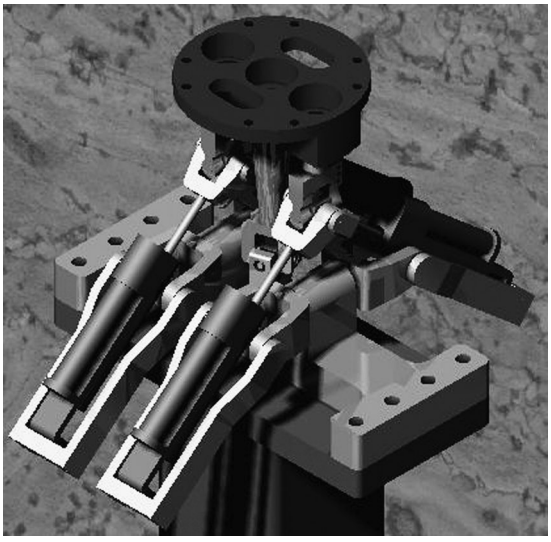

Figure 1. A schematic of the hydraulic shoulder manipulator.

Figure 2. The hydraulic shoulder in movement.

In these robots, the end-effector is connected to the base through several closed kinematic chains. The motivation behind using these types of robot manipulators was to compensate for the shortcomings of conventional serial manipulators such as low precision, stiffness and load-carrying capability. However, they have their own disadvantages, which are mainly smaller workspace and many singular configurations. The hydraulic shoulder, having a parallel structure, has the general features of these structures. It can be considered as a shoulder for a lightweight 7-d.o.f. robotic arm, which can carry loads several times its own weight. Simple elements, used in this design, add to its lightness and simplicity. The workspace of such a mechanism can be considered as part of a spherical surface. The orientation angles are limited to vary between $-\pi/6$ and $\pi/6$.

Figure 2 shows the hydraulic shoulder in a twisted configuration. No sensors are available for measuring the orientation angles of the moving platform. This fact justifies the importance of the forward kinematic map as a key element in feedback position control of the shoulder with the LVDT position sensors used as the only source of measurement in such a control scheme. A complete analysis of such a carefully designed mechanism will provide the required means to better understand the characteristics of the structure, the required performance and the corresponding control algorithms.

3. KINEMATICS

Figure 3 depicts a geometric model for the hydraulic shoulder manipulator, which will be used for its kinematics derivation. The parameters used in kinematics can

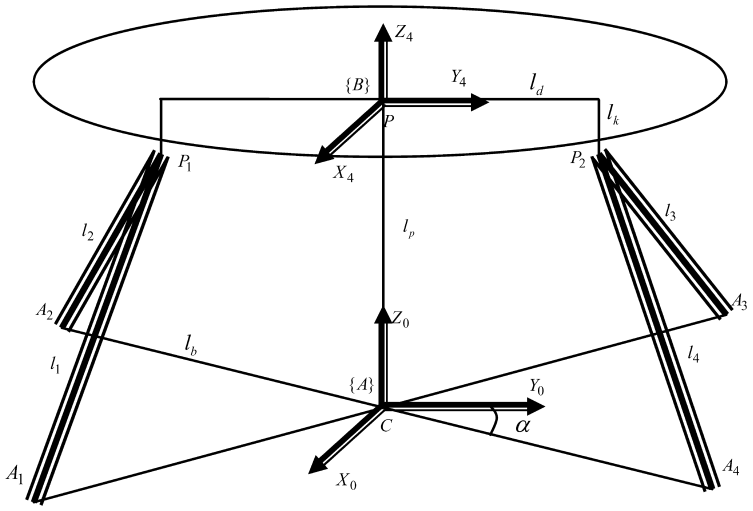

Figure 3. A geometric model for the hydraulic shoulder manipulator.

be defined as:

$$l_b = \left\|\overrightarrow{\mathrm{CA}_i}\right\|, \quad l_p = \left\|\overrightarrow{\mathrm{CP}}\right\|, \quad l_d = \left\|\overrightarrow{\mathrm{PP}_i}\right\|_{y_4}, \quad l_k = \left\|\overrightarrow{\mathrm{PP}_i}\right\|_{z_4},$$

where α is the angle between CA_4 and y_0, C is the center of the reference frame, P is the center of the moving plate, l_i are actuator lengths, P_i are moving endpoints of the actuators and A_i are fixed endpoints of the actuators. Two coordinate frames are defined for the purpose of analysis. The base coordinate frame {A}: $x_0y_0z_0$ is attached to the fixed base at point C (rotation center) with its z_0-axis perpendicular to the plane defined by the actuator base points $\mathrm{A}_1\mathrm{A}_2\mathrm{A}_3\mathrm{A}_4$ and an x_0-axis parallel to the bisector of angle $\angle\mathrm{A}_1\mathrm{CA}_4$. The second coordinate frame {B}: $x_4y_4z_4$ is attached to the center of the moving platform P with its z-axis perpendicular to the line defined by the actuators moving end points ($\mathrm{P}_1\mathrm{P}_2$) along the passive limb. Note that we have assumed that the actuator fixed endpoints lie on the same plane as the rotation center C. The position of the moving platform center P is defined by:

$$^{\mathrm{A}}p = [p_x, p_y, p_z]^{\mathrm{T}}. \tag{1}$$

Also, a rotation matrix $^{\mathrm{A}}R_{\mathrm{B}}$ is used to define the orientation of the moving platform with respect to the base frame:

$$\begin{aligned} {}^{\mathrm{A}}R_{\mathrm{B}} &= R_z(\theta_z)R_y(\theta_y)R_x(\theta_x) \\ &= \begin{bmatrix} c\theta_z c\theta_y & c\theta_z s\theta_y s\theta_x - s\theta_z c\theta_x & c\theta_z s\theta_y c\theta_x + s\theta_z s\theta_x \\ s\theta_z c\theta_y & s\theta_z s\theta_y s\theta_x + c\theta_z c\theta_x & s\theta_z s\theta_y c\theta_x - c\theta_z s\theta_x \\ -s\theta_y & c\theta_y s\theta_x & c\theta_y c\theta_x \end{bmatrix}, \end{aligned} \tag{2}$$

where θ_x, θ_y and θ_z are the orientation angles of the moving platform denoting rotations of the moving frame about the fixed x-, y- and z-axes, respectively. Also $c\theta$ and $s\theta$ denote $\cos(\theta)$ and $\sin(\theta)$, respectively.

With the above definitions, the 4×4 transformation matrix ${}^{\mathrm{A}}T_{\mathrm{B}}$ is easily found to be:

$$ {}^{\mathrm{A}}T_{\mathrm{B}} = \begin{bmatrix} {}^{\mathrm{A}}R_{\mathrm{B}} & {}^{\mathrm{A}}p \\ \mathbf{0} & 1 \end{bmatrix}. \tag{3} $$

Hence, the position and orientation of the moving platform are completely defined by six variables, from which only three orientation angles θ_x, θ_y and θ_z are independently specified as the task space variables of the hydraulic shoulder.

3.1. Inverse kinematics

In modeling the inverse kinematics of the hydraulic shoulder we must determine actuator lengths (l_i) as the actuator space variables given the task space variables θ_x, θ_y and θ_z as the orientation angles of the moving platform. First, note that the passive limb connecting the center of the rotation to the moving platform can be viewed as a 3-d.o.f. open-loop chain by defining three joint variables θ_1, θ_2 and θ_3 as the joint space variables of the hydraulic shoulder. Hence, applying the Denavit–Hartenberg (D–H) convention, the transformation ${}^{\mathrm{A}}T_{\mathrm{B}}$ can also be written as:

$$ {}^{\mathrm{A}}T_{\mathrm{B}} = {}^{\mathrm{A}}T_1(\theta_1) \cdot {}^{1}T_2(\theta_2) \cdot {}^{2}T_3(\theta_3) \cdot {}^{3}T_{\mathrm{B}}. \tag{4} $$

The D–H transformation matrices ${}^{i}T_j$ are computed using the coordinate systems for the passive limb in Fig. 4, according to the D–H convention. As shown in Fig. 4, the x_0-axis of frame {A} points along the first joint axis of the passive limb, the first

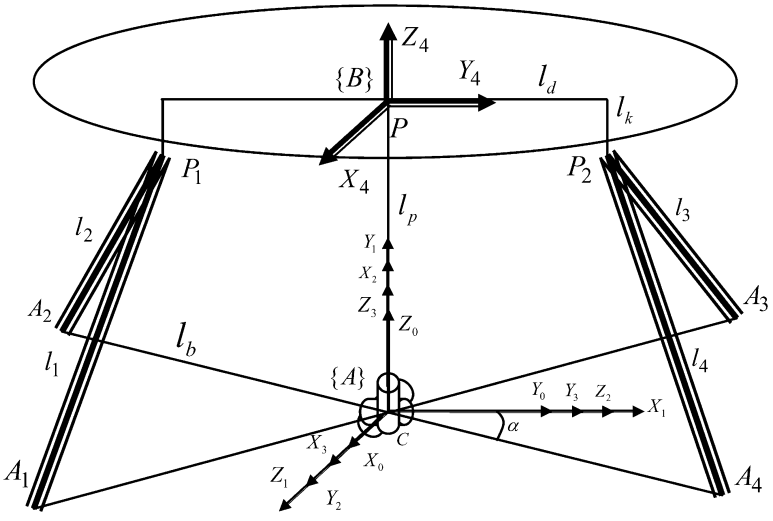

Figure 4. D–H Frame attachments for the passive supporting limb.

Table 1.
D–H parameters for the passive supporting limb

i	α_{i-1}	a_{i-1}	d_i	θ_i
1	90°	0	0	θ_1
2	90°	0	0	θ_2
3	90°	0	0	θ_3
B	0	0	l_p	0

link frame is attached to the first moving link with its x_1-axis pointing along the second joint axis of the passive limb, the second link frame is attached to the second moving link with its x_2-axis pointing along the third joint axis of the passive limb and the third link frame is attached to the moving platform in accordance with the D–H convention. Using the above frames, the D–H parameters of the passive limb are found as in Table 1.

Using the D–H parameters in Table 1, the D–H transformation matrices in (4) can be found as:

$$
\begin{aligned}
{}^{\mathrm{A}}T_1 &= \begin{bmatrix} c\theta_1 & -s\theta_1 & 0 & 0 \\ 0 & 0 & -1 & 0 \\ s\theta_1 & c\theta_1 & 0 & 0 \\ 0 & 0 & 0 & 1 \end{bmatrix}, \quad {}^{1}T_2 = \begin{bmatrix} c\theta_2 & -s\theta_2 & 0 & 0 \\ 0 & 0 & -1 & 0 \\ s\theta_2 & c\theta_2 & 0 & 0 \\ 0 & 0 & 0 & 1 \end{bmatrix}, \\
{}^{2}T_3 &= \begin{bmatrix} c\theta_3 & -s\theta_3 & 0 & 0 \\ 0 & 0 & -1 & 0 \\ s\theta_3 & c\theta_3 & 0 & 0 \\ 0 & 0 & 0 & 1 \end{bmatrix}, \quad {}^{3}T_{\mathrm{B}} = \begin{bmatrix} 1 & 0 & 0 & 0 \\ 0 & 1 & 0 & 0 \\ 0 & 0 & 1 & l_p \\ 0 & 0 & 0 & 1 \end{bmatrix}.
\end{aligned} \tag{5}
$$

Substituting (5) into (4) yields:

$$
{}^{\mathrm{A}}T_{\mathrm{B}} = \begin{bmatrix} {}^{\mathrm{A}}R_{\mathrm{B}} & {}^{\mathrm{A}}p \\ \mathbf{0} & 1 \end{bmatrix}, \tag{6}
$$

where:

$$
{}^{\mathrm{A}}R_{\mathrm{B}} = \begin{bmatrix} c\theta_1 c\theta_2 c\theta_3 + s\theta_1 s\theta_3 & -c\theta_1 c\theta_2 s\theta_3 + s\theta_1 c\theta_3 & c\theta_1 s\theta_2 \\ -s\theta_2 c\theta_3 & s\theta_2 s\theta_3 & c\theta_2 \\ s\theta_1 c\theta_2 c\theta_3 - c\theta_1 s\theta_3 & -s\theta_1 c\theta_2 s\theta_3 - c\theta_1 c\theta_3 & s\theta_1 s\theta_2 \end{bmatrix}, \tag{7}
$$

and

$$
{}^{\mathrm{A}}p = \begin{bmatrix} l_p c\theta_1 s\theta_2 & l_p c\theta_2 & l_p s\theta_1 s\theta_2 \end{bmatrix}^{\mathrm{T}}. \tag{8}
$$

For the inverse kinematics, the three independent orientation angles in (2) are given. Hence, equating (2)–(7) yields:

$$
\theta_2 = \cos^{-1}\left({}^{\mathrm{A}}R_{\mathrm{B}(2,3)}\right) = \cos^{-1}(s\theta_z s\theta_y c\theta_x - c\theta_z s\theta_x). \tag{9}
$$

Once θ_2 is known, we can solve for θ_1 and θ_3 as:

$$\theta_1 = A\tan 2\left(\frac{{}^{\mathrm{A}}R_{\mathrm{B}(3,3)}}{s\theta_2}, \frac{{}^{\mathrm{A}}R_{\mathrm{B}(1,3)}}{s\theta_2}\right), \tag{10}$$

and:

$$\theta_3 = A\tan 2\left(\frac{{}^{\mathrm{A}}R_{\mathrm{B}(2,2)}}{s\theta_2}, \frac{-{}^{\mathrm{A}}R_{\mathrm{B}(2,1)}}{s\theta_2}\right), \tag{11}$$

provided that $s\theta_2 \neq 0$. Having the joint space variables θ_1, θ_2 and θ_3 in hand, we can easily solve for the position of the moving platform using (8). Now, in order to find the actuator lengths, we write a kinematic vector-loop equation for each actuated limb as:

$$L_i = l_i \cdot s_i = {}^{\mathrm{A}}p + {}^{\mathrm{A}}R_{\mathrm{B}}\,{}^{\mathrm{B}}p_i - a_i, \tag{12}$$

where l_i is the length of the ith actuated limb and s_i is a unit vector pointing along the direction of the ith actuated limb. Also, ${}^{\mathrm{A}}p$ is the position vector of the moving platform and ${}^{\mathrm{A}}R_{\mathrm{B}}$ is its rotation matrix. Vectors a_i and ${}^{\mathrm{B}}p_i$ denote the fixed end points of the actuators (A_i) in the base frame and the moving end points of the actuators respectively, written as:

$$\begin{aligned}
a_1 &= {}^{\mathrm{A}}A_1 = (l_b\sin\alpha \quad -l_b\cos\alpha \quad 0)^{\mathrm{T}}\\
a_2 &= {}^{\mathrm{A}}A_2 = (-l_b\sin\alpha \quad -l_b\cos\alpha \quad 0)^{\mathrm{T}}\\
a_3 &= {}^{\mathrm{A}}A_3 = (-l_b\sin\alpha \quad l_b\cos\alpha \quad 0)^{\mathrm{T}}\\
a_4 &= {}^{\mathrm{A}}A_4 = (l_b\sin\alpha \quad l_b\cos\alpha \quad 0)^{\mathrm{T}},
\end{aligned} \tag{13}$$

and

$$\begin{aligned}
{}^{\mathrm{B}}p_1 &= (0 \quad -l_d \quad -l_k)^{\mathrm{T}}\\
{}^{\mathrm{B}}p_2 &= (0 \quad l_d \quad -l_k)^{\mathrm{T}}.
\end{aligned} \tag{14}$$

Hence, the actuator lengths l_i can be easily computed by dot multiplying (12) with itself to yield:

$$L_i^{\mathrm{T}}.L_i = l_i^2 = \left[{}^{\mathrm{A}}p + {}^{\mathrm{A}}R_{\mathrm{B}}\,{}^{\mathrm{B}}p_i - a_i\right]^{\mathrm{T}}\left[{}^{\mathrm{A}}p + {}^{\mathrm{A}}R_{\mathrm{B}}\,{}^{\mathrm{B}}p_i - a_i\right]. \tag{15}$$

Writing (15) four times with the corresponding parameters given in (7), (8), (13) and (14), and simplifying the results yields:

$$l_1^2 = k_1 + k_2c\theta_2 + k_3c\theta_1s\theta_2 + k_4(s\theta_1c\theta_3 - c\theta_1c\theta_2s\theta_3) + k_5s\theta_2s\theta_3 \tag{16a}$$

$$l_2^2 = k_1 + k_2c\theta_2 - k_3c\theta_1s\theta_2 - k_4(s\theta_1c\theta_3 - c\theta_1c\theta_2s\theta_3) + k_5s\theta_2s\theta_3 \tag{16b}$$

$$l_3^2 = k_1 - k_2c\theta_2 - k_3c\theta_1s\theta_2 + k_4(s\theta_1c\theta_3 - c\theta_1c\theta_2s\theta_3) + k_5s\theta_2s\theta_3 \tag{16c}$$

$$l_4^2 = k_1 - k_2c\theta_2 + k_3c\theta_1s\theta_2 - k_4(s\theta_1c\theta_3 - c\theta_1c\theta_2s\theta_3) + k_5s\theta_2s\theta_3, \tag{16d}$$

where:

$$\begin{aligned} k_1 &= l_b^2 + l_d^2 + (l_p - l_k)^2 \\ k_2 &= 2l_b(l_p - l_k)\cos(\alpha) \\ k_3 &= -2l_b(l_p - l_k)\sin(\alpha) \\ k_4 &= 2l_b l_d \sin(\alpha) \\ k_5 &= -2l_b l_d \cos(\alpha). \end{aligned} \tag{17}$$

Finally, the actuator lengths are given by the square roots of (16), yielding actuator space variables as the unknowns of the inverse kinematics problem.

3.2. Forward kinematics

Forward kinematics is undoubtedly a basic element in modeling and control of the manipulator. In forward kinematic analysis of the hydraulic shoulder, we shall find all the possible orientations of the moving platform for a given set of actuated limb lengths. Equation (16) can also be used for the forward kinematics of the hydraulic shoulder, but with the actuator lengths as the input variables. In fact, we have four non-linear equations to solve for three unknowns. First, we try to express the moving platform position and orientation in terms of the joint variables θ_1, θ_2 and θ_3 using (7) and (8). As is obvious from (16), the only unknowns are the joint variables θ_1, θ_2 and θ_3, since actuator lengths are given and all other parameters are determined by the geometry of the manipulator. Hence, we must solve the equations for six unknowns from which only three are independent. Summing (16a) and (16b) we get:

$$l_1^2 + l_2^2 = 2k_1 + 2k_2 c\theta_2 + 2k_5 s\theta_2 s\theta_3. \tag{18}$$

Similarly adding (16c) and (16d) yields:

$$l_3^2 + l_4^2 = 2k_1 - 2k_2 c\theta_2 + 2k_5 s\theta_2 s\theta_3. \tag{19}$$

Subtracting (19) from (18), we can solve for $c\theta_2$ as:

$$c\theta_2 = \frac{l_1^2 + l_2^2 - l_3^2 - l_4^2}{4k_2}. \tag{20}$$

Substituting (20) into the trigonometric identity $s\theta_2^2 + c\theta_2^2 = 1$, we get:

$$s\theta_2 = \pm\sqrt{1 - c\theta_2^2}. \tag{21}$$

Having $s\theta_2$ and $c\theta_2$ in hand, we can solve for $s\theta_3$ from (18) as:

$$s\theta_3 = \frac{l_1^2 + l_2^2 - 2k_1 - 2k_2 c\theta_2}{2k_5 s\theta_2}. \tag{22}$$

Similarly:

$$c\theta_3 = \pm\sqrt{1 - s\theta_3^2}. \tag{23}$$

To solve for the remaining unknowns, $c\theta_1$ and $s\theta_1$, we sum (16b) and (16c) to get:

$$l_2^2 + l_3^2 = 2k_1 - 2k_3 c\theta_1 s\theta_2 + 2k_5 s\theta_2 s\theta_3. \tag{24}$$

Having computed $s\theta_2$ and $s\theta_3$, we obtain:

$$c\theta_1 = \frac{2k_1 + 2k_5 s\theta_2 s\theta_3 - l_2^2 - l_3^2}{2k_3 s\theta_2}. \tag{25}$$

Finally:

$$s\theta_1 = \pm\sqrt{1 - c\theta_1^2}. \tag{26}$$

Hence, the joint space variables are given by:

$$\theta_1 = A\tan 2(s\theta_1, c\theta_1), \quad \theta_2 = A\tan 2(s\theta_2, c\theta_2), \quad \theta_3 = A\tan 2(s\theta_3, c\theta_3). \tag{27}$$

Also, the moving platform position ${}^{\mathrm{A}}p$ and orientation ${}^{\mathrm{A}}R_{\mathrm{B}}$ are found using (7) and (8). The final step is to solve for the orientation angles θ_x, θ_y and θ_z using (3) which completes the solution process to the forward kinematics of the hydraulic shoulder. It should be noted that there are some additional erroneous solutions to the forward kinematics as stated above due to several square roots involved in the process. These solutions must be identified and omitted. Another important assumption made in our solution procedure was that all four actuator fixed endpoints are coplanar, just as the actuator moving endpoints.

4. MECHANISM JACOBIAN

The Jacobian matrix of a 3-d.o.f. parallel manipulator relates the task space linear or angular velocity to the vector of actuated joint rates in a way that it corresponds to the inverse Jacobian of a serial manipulator. In this section, we derive the Jacobian for the hydraulic shoulder as a basic requirement for singularity analysis, stiffness analysis and position control of this manipulator. For the Jacobian analysis of the hydraulic shoulder, we must find a relationship between the angular velocity of the moving platform, $\boldsymbol{\omega}$, and the vector of limb rates as the actuator space variables, $\dot{\mathbf{l}} = [\dot{l}_1 \quad \dot{l}_2 \quad \dot{l}_3 \quad \dot{l}_4]^{\mathrm{T}}$, so that:

$$\dot{\mathbf{l}} = J\boldsymbol{\omega}. \tag{28}$$

From the above definition, it is easily observed that the Jacobian for the hydraulic shoulder will be a 4×3 rectangular matrix as expected, regarding the mechanism as an actuator redundant manipulator. Using the same idea of mapping between actuator, joint and task space, we find that the Jacobian depends on the actuated limbs, as well as the passive supporting limb. Therefore, we first derive a 4×6 Jacobian, J_{l}, relating the six-dimensional velocity of the moving platform, $\mathbf{v}$, to the vector of actuated limb rates, $\dot{\mathbf{l}}$. Then, we find the 6×3 Jacobian of the passive

supporting limb, J_{p}. The Jacobian of the hydraulic shoulder will be finally derived as:

$$J = J_{\mathrm{l}} J_{\mathrm{p}}. \tag{29}$$

4.1. Jacobian of the actuated limbs

The Jacobian of the actuated limbs, J_{l}, relates the six-dimensional velocity of the moving platform, $\mathbf{v}$, to the vector of actuated limb rates, $\dot{\mathbf{l}}$, such that:

$$\dot{\mathbf{l}} = J_{\mathrm{l}} \mathbf{v}. \tag{30}$$

We can write the six-dimensional moving platform velocity as:

$$\mathbf{v} = \begin{bmatrix} {}^{\mathrm{A}}\dot{p} \\ \boldsymbol{\omega} \end{bmatrix} = \begin{bmatrix} \dot{p}_x & \dot{p}_y & \dot{p}_z & \omega_x & \omega_y & \omega_z \end{bmatrix}^{\mathrm{T}}, \tag{31}$$

where ${}^{\mathrm{A}}\dot{p}$ is the velocity of the moving platform center and $\boldsymbol{\omega}$ is the angular velocity of the moving platform. Differentiating the kinematic vector-loop equation (12) with respect to time we get:

$$\dot{l}_i s_i + (\omega_i \times s_i) l_i = {}^{\mathrm{A}}\dot{p} + \boldsymbol{\omega} \times {}^{\mathrm{A}}R_{\mathrm{B}}\, {}^{\mathrm{B}}p_i, \tag{32}$$

where ω_i is the angular velocity of the ith limb written in the base frame. Dot multiplying (32) by s_i we have:

$$\dot{l}_i = s_i^{\mathrm{T}} \cdot {}^{\mathrm{A}}\dot{p} + ({}^{\mathrm{A}}R_{\mathrm{B}}\, {}^{\mathrm{B}}p_i \times s_i)^{\mathrm{T}} \boldsymbol{\omega}, \tag{33}$$

writing the above equation four times for each actuated limb and comparing the result to (30) gives the actuated limbs Jacobian as:

$$J_{\mathrm{l}} = \begin{bmatrix} s_1^{\mathrm{T}} & \left({}^{\mathrm{A}}R_{\mathrm{B}}\, {}^{\mathrm{B}}p_1 \times s_1\right)^{\mathrm{T}} \\ s_2^{\mathrm{T}} & \left({}^{\mathrm{A}}R_{\mathrm{B}}\, {}^{\mathrm{B}}p_2 \times s_2\right)^{\mathrm{T}} \\ s_3^{\mathrm{T}} & \left({}^{\mathrm{A}}R_{\mathrm{B}}\, {}^{\mathrm{B}}p_1 \times s_3\right)^{\mathrm{T}} \\ s_4^{\mathrm{T}} & \left({}^{\mathrm{A}}R_{\mathrm{B}}\, {}^{\mathrm{B}}p_2 \times s_4\right)^{\mathrm{T}} \end{bmatrix}_{4\times 6}. \tag{34}$$

4.2. Jacobian of the passive limb

In order to find the manipulator Jacobian, we need to find a relationship between the six-dimensional velocity vector of the moving platform, $\mathbf{v}$, and the angular velocity of the moving platform, $\boldsymbol{\omega}$. First, by differentiating (8) with respect to time we get:

$${}^{\mathrm{A}}\dot{p} = \begin{bmatrix} -l_p s\theta_1 s\theta_2 & l_p c\theta_1 c\theta_2 & 0 \\ 0 & -l_p s\theta_2 & 0 \\ l_p c\theta_1 s\theta_2 & l_p s\theta_1 c\theta_2 & 0 \end{bmatrix} \dot{\boldsymbol{\theta}}, \tag{35}$$

where $\dot{\boldsymbol{\theta}} = [\,\dot{\theta}_1 \quad \dot{\theta}_2 \quad \dot{\theta}_3\,]^{\mathrm{T}}$ is the vector of the passive joint rates. The angular velocity of the moving platform can also be expressed as:

$$\boldsymbol{\omega} = {}^{\mathrm{A}}\dot{R}_{\mathrm{B}}\,{}^{\mathrm{A}}R_{\mathrm{B}}^{-1}. \tag{36}$$

Substituting ${}^{\mathrm{A}}R_{\mathrm{B}}$ from (7) and computing (36), we have:

$$\boldsymbol{\omega} = \begin{bmatrix} 0 & s\theta_1 & c\theta_1 s\theta_2 \\ -1 & 0 & c\theta_2 \\ 0 & -c\theta_1 & s\theta_1 s\theta_2 \end{bmatrix} \dot{\boldsymbol{\theta}}. \tag{37}$$

Solving (37) for $\dot{\boldsymbol{\theta}}$ and substituting it in (35) yields:

$${}^{\mathrm{A}}\dot{p} = \begin{bmatrix} 0 & l_p s\theta_1 s\theta_2 & -l_p c\theta_2 \\ -l_p s\theta_1 s\theta_2 & 0 & l_p c\theta_1 s\theta_2 \\ l_p c\theta_2 & -l_p c\theta_1 s\theta_2 & 0 \end{bmatrix} \boldsymbol{\omega}. \tag{38}$$

Complementing (38) with the identity map $\boldsymbol{\omega} = I_3\boldsymbol{\omega}$, we finally obtain:

$$\mathbf{v} = \begin{bmatrix} {}^{\mathrm{A}}\dot{p} \\ \boldsymbol{\omega} \end{bmatrix} = J_p\boldsymbol{\omega}, \tag{39}$$

where:

$$J_p = \begin{bmatrix} 0 & l_p s\theta_1 s\theta_2 & -l_p c\theta_2 \\ -l_p s\theta_1 s\theta_2 & 0 & l_p c\theta_1 s\theta_2 \\ l_p c\theta_2 & -l_p c\theta_1 s\theta_2 & 0 \\ 1 & 0 & 0 \\ 0 & 1 & 0 \\ 0 & 0 & 1 \end{bmatrix}_{6\times 3}. \tag{40}$$

Having J_1 and J_p in hand, the hydraulic shoulder Jacobian $J_{4\times 3}$ will be easily found using (29).

5. SINGULARITY ANALYSIS

In this section, singularity analysis of the hydraulic shoulder is performed, based on the Jacobian of the manipulator. A singular configuration describes a manipulator posture that results in an instantaneous change in the mobility of the manipulator. These are undesirable postures that should be recognized and avoided during the design, planning and control. Researchers have introduced various approaches to determine and classify the singularities of parallel manipulators. All of these approaches are mostly based on a Jacobian analysis, since the Jacobian degenerates when the manipulator is in a singular configuration. Gosselin and Angeles [18] were perhaps the first to define and study singularities of closed kinematic chains [19].

According to their classification, singularities for parallel manipulators can be categorized into three types.

The first type of singularity (an inverse kinematic singularity) occurs at the workspace boundaries and can be avoided by motion planning. The second type of singularity (a direct kinematic singularity) results in additional degrees of freedom at the end-effector and the mechanism cannot maintain its static equilibrium upon external forces. Singularity of the third type occurs when the manipulator is in a posture that produces a singularity of the first and the second type simultaneously. Generally, this type of singularity can occur only in manipulators with special kinematic architecture and should be avoided in the design stage. Hence, the direct kinematic singularity is the only type that lies within the workspace of the manipulator and should be carefully avoided. For a redundant parallel manipulator, in general, singularities will occur if the Jacobian rank is lower than m, the number of d.o.f. of the moving platform, or equivalently if:

$$\det(M) = 0, \quad \forall M \in \{m \times m \text{ submatrices of } J\}. \tag{41}$$

It should be noted that only $n-m+1$ conditions from (41) are independent, where n is the number of actuated joints. Hence, singularities are found at the intersection of $n-m+1$ hypersurfaces resulting in a lower dimensional manifold with a dimension of $m-(n-m+1) = m-1-n_{\mathrm{R}}$ in the task space, where n_{R} is the number of redundant actuators. Thus, actuator redundancy can be effectively used to reduce or even eliminate the singularities in the workspace.

For the hydraulic shoulder manipulator, as shown in the previous section, the linear velocities of the actuators $\dot{\mathbf{l}}$ are related to the angular velocity of the moving platform $\boldsymbol{\omega}$ by (28), in which J was the Jacobian matrix of the hydraulic shoulder. Thus singularities are characterized by the rank deficiency of J. Such a case occurs only if the determinants of all 3×3 minors of J are identically zero. These square minors correspond to the Jacobian matrices of the hydraulic shoulder with one of the actuating limbs removed. Therefore, the redundant manipulator will be in a singular configuration only if all the non-redundant structures resulted by suppressing one of the actuating limbs are in a singular configuration. Such a case will not occur in the workspace of the hydraulic shoulder owing to the specific design of the mechanism [14]. In fact, one of the remarkable features of adding the fourth actuator is the elimination of the loci of singularities. Figure 5 shows the determinants of the four minor Jacobian matrices, computed in the workspace of the manipulator, defined as *DM1–DM4*. It should be noted, that in computing *DM1*, *DM2*, *DM3* and *DM4*, limbs 4, 3, 2 and 1 were removed, respectively, to obtain the corresponding non-redundant structure. As it is shown in Fig. 5, the values of the minor Jacobian matrices vary throughout the spherical surface of the workspace of the manipulator. However, they do not reach to a minimum simultaneously at a particular configuration. To see this more clearly in Fig. 5, notice that, for example, at the configurations where *DM2* becomes minimum (red) *DM1* and *DM3* get their mid-value (cyan–yellow), and *DM4* possess its high value (blue). Further-

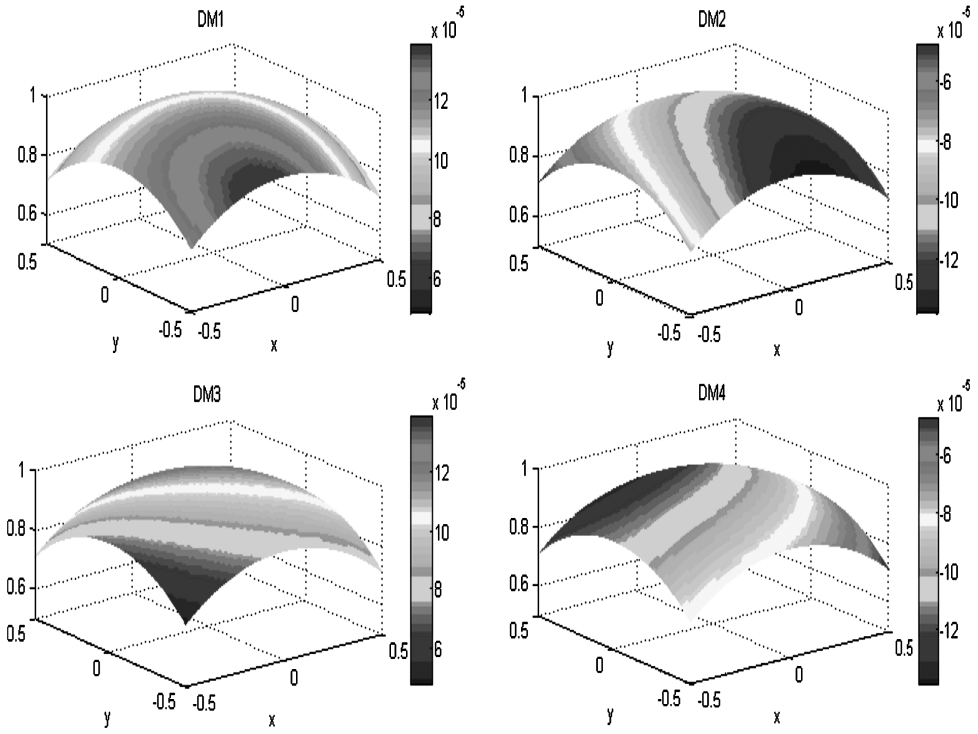

Figure 5. Minor determinants for the non-redundant structures; in computing *DM1–DM4*, limbs 4, 3, 2 and 1 were removed, respectively.

more, similar patterns can be observed at configurations where the other Jacobian minors becomes minimum. Therefore, there exists no configuration throughout the entire workspace of the hydraulic shoulder where all minor Jacobian matrices reach their minimum simultaneously. Moreover, the possibility of getting into a singular configuration is increased when one of the redundant actuators is removed. Hence, the designer's claim that the mechanism is singularity-free throughout its whole workspace is verified. Note that although this analysis is performed for our specific parallel manipulator, minor Jacobian matrices can be used in a similar fashion for singularity analysis of other parallel manipulators. In cases where there is no redundancy in actuation, similar analysis can be performed to obtain singular configurations and in case one of the actuators malfunctions in a redundant manipulator, its effect on the singularity of the manipulator can be examined in detail.

6. STIFFNESS ANALYSIS

The stiffness of a parallel manipulator at a given point of its workspace can be characterized by its stiffness matrix, which relates the forces and torques applied to

the moving platform in the Cartesian space to the corresponding linear and angular Cartesian displacements. The stiffness of a manipulator is known to have a direct impact on its position accuracy, and generally depends on several factors like the limbs size and material, actuators, and the control system [20]. Several researchers have studied the stiffness of parallel manipulators regarding either the stiffness properties of a specific design or different approaches of compliance control of parallel manipulators [21, 22].

In this section, a detail Cartesian stiffness analysis is performed for the hydraulic shoulder resulting in the stiffness matrix of the mechanism as the basis for developing relating control strategies. In fact, this analysis could be a critical starting point for further research in this field such as accurate position control or the problem of controlling the manipulator in an environment with kinematic and force constraints, in which a desired and appropriate stiffness should be synthesized to be used in various schemes of stiffness control. Furthermore, the stiffness matrix gives information on some important kinematic properties of the manipulator such as dexterity or manipulability [21]. The analysis of the Cartesian stiffness is based on the definition described in Ref. [23]. Actuator stiffness has been considered as the main source of stiffness.

Let $f = [f_1 \;\; f_2 \;\; f_3 \;\; f_4]^{\mathrm{T}}$ be the vector of actuated joint forces and $\Delta\ell = [\Delta\ell_1 \;\; \Delta\ell_2 \;\; \Delta\ell_3 \;\; \Delta\ell_4]^{\mathrm{T}}$ be the corresponding vector of virtual displacements of actuated joints. Then, we can relate $\Delta\ell$ to f by a $n \times n$ diagonal matrix $K_{\mathrm{a}} = \mathrm{diag}[k_1, \ldots, k_n]$, as follows:

$$f = K_{\mathrm{a}} \Delta\ell. \tag{42}$$

In fact, for the hydraulic shoulder, K_{a} is a 4×4 diagonal matrix with actuators stiffness constants on its main diagonal elements. From the definition of the Jacobian in (28), we have:

$$\Delta\ell = J \Delta\theta, \tag{43}$$

in which $\Delta\theta = [\Delta\theta_x \;\; \Delta\theta_y \;\; \Delta\theta_z]^{\mathrm{T}}$ is the vector of the virtual angular displacement of the moving platform. Also, the three-dimensional vector of end-effector output forces, $\tau = [\tau_x \;\; \tau_y \;\; \tau_z]^{\mathrm{T}}$ is related to the vector of actuated joint forces by the principle of virtual work as:

$$\tau = J^{\mathrm{T}} f. \tag{44}$$

Substituting (43) into (42) we obtain:

$$f = K_{\mathrm{a}} J \Delta\theta. \tag{45}$$

Finally, substituting (45) into (44), yields:

$$\tau = K \Delta\theta, \tag{46}$$

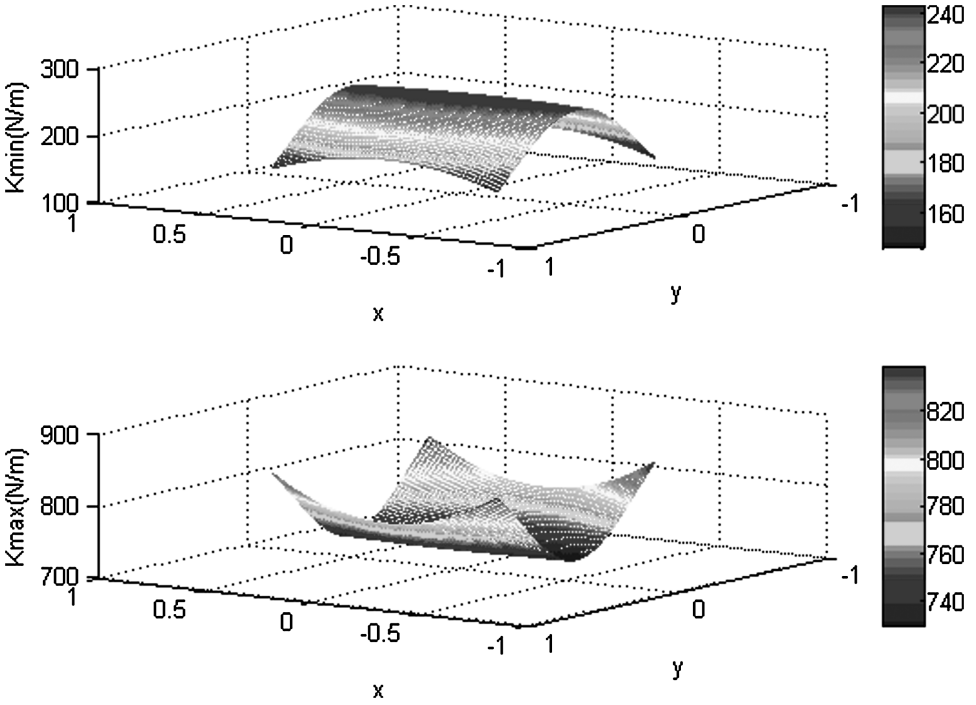

Figure 6. Minimum and maximum stiffness mappings.

where:

$$K = J^{\mathrm{T}} K_{\mathrm{a}} J, \tag{47}$$

is called the stiffness matrix of the hydraulic shoulder manipulator. As it is obvious from (47), the stiffness matrix is configuration dependent. For a given configuration of the moving platform the eigenvalue of the stiffness matrix will represent the stiffness of the hydraulic shoulder in the corresponding eigenvector direction. Twist vectors in fact represent these directions. Similarly, minimum and maximum stiffness mappings could be obtained using the corresponding eigenvalues and eigenvectors. These maps are shown in Fig. 6, assuming equal stiffness constants of 10^5 N/m for all the actuators modeled as linear springs. Moreover, the square root of the ratio of the smallest eigenvalue to the largest one indicates the reciprocal of the condition number of the Jacobian matrix, which is also a measure of the dexterity of the manipulator. It is observed that actuator redundancy has improved the Cartesian stiffness of the hydraulic shoulder. This is shown in Fig. 7, where the Euclidean norms of the stiffness matrix are computed for the redundant and non-redundant manipulator by suppressing one of the limbs. It is clearly observed in Fig. 7 that loosing one limb actuation significantly reduces the Cartesian stiffness of the manipulator.

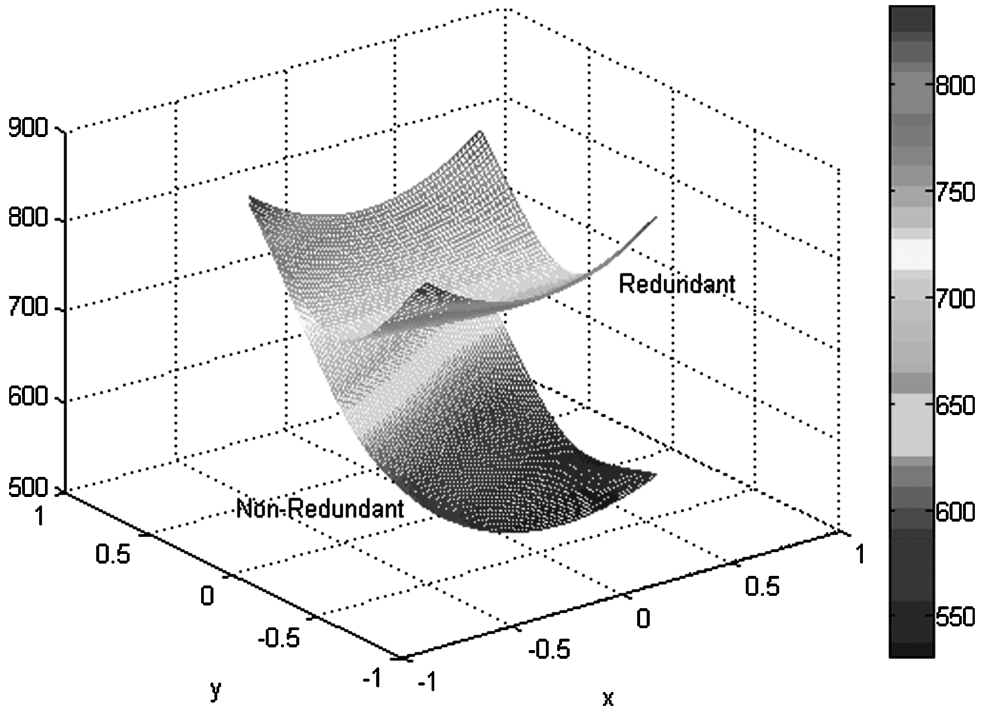

Figure 7. Comparison of Cartesian stiffness for the redundant and non-redundant structure.

7. CONCLUSIONS

In this paper, kinematic modeling, and singularity and stiffness analysis of a 3-d.o.f. redundant parallel manipulator has been performed in detail. Using the idea of inherent kinematic chains formed in parallel manipulators, both inverse and forward kinematics of the hydraulic shoulder are fully developed, and a closed-form solution for the forward kinematic map is derived as a basic need for closed-loop position control of the manipulator. Furthermore, the closed form of the mechanism Jacobian is derived and a singularity analysis is performed based on the computed Jacobian. In this study the determinant of the minor Jacobian matrices are used as a measure of singularity, in which this is computed from the non-redundant structures by removing the redundant actuator. It is observed that the values of the determinant of the minor Jacobian matrices do not reach their minimum simultaneously at a particular configuration and, hence, the hydraulic shoulder workspace is singular free. Moreover, removing one of the redundant actuators increases the possibility of getting into a singular configuration. Finally, the stiffness mapping of the manipulator is derived and its configuration dependence is analyzed. It is shown that the actuator redundancy in the mechanism is the major element to improve the Cartesian stiffness of the hydraulic shoulder and by loosing one limb actuation the stiffness of the manipulator reduces significantly.

REFERENCES

1. J. P. Merlet, Still a long way to go on the road for parallel mechanisms, in: *Proc. ASME 2002 DETC Conf.*, Montreal (2002).
2. J. P. Merlet, Parallel robots: open problems, in: *9th Int. Symp. of Robotics Research*, Snowbird, UT (1999).
3. S. Joshi and L. W. Tsai, The kinematics of a class of 3-DOF, 4-limbed parallel manipulators, *Trans. ASME* **125**, 52–60 (2003).
4. S. Joshi and L. W. Tsai, A comparison study of two 3-DOF parallel manipulators: one with three and the other with four supporting limbs, *IEEE Trans. Robotics Automat.* **19**, 200–209 (2003).
5. L. Baron and J. Angeles, The kinematic decoupling of parallel manipulators using joint-sensor data, *IEEE Trans. Robotics Automat.* **16**, 644–651 (2000).
6. J. P. Merlet, Closed-form resolution of the direct kinematics of parallel manipulators using extra sensors data, in: *Proc. IEEE Int. Conf. on Robotics and Automation*, pp. 200–204 (1993).
7. J. P. Merlet, Direct kinematics of planar parallel manipulators, in: *Proc. IEEE Int. Conf. on Robotics and Automation*, MN, pp. 3744–3749 (1996).
8. S. K. Song and D. S. Kwon, Efficient formulation approach for the forward kinematics of the 3–6 Stewart–Gough platform, in: *Proc. Int. Conf. on Intelligent Robots and Systems*, HI, pp. 1688–1693 (2001).
9. I. A. Bonev, J. Ryu, S.-G. Kim and S.-K. Lee, A closed-form solution to the direct kinematics of nearly general parallel manipulators with optimally located three linear extra sensors, *IEEE Trans. Robotics Automat.* **17**, 148–156 (2001).
10. B. Siciliano, The tricept robot: inverse kinematics, manipulability analysis and closed-loop direct kinematics algorithm, *Robotica* **17**, 437–445 (1999).
11. A. Fattah and G. Kasaei, Kinematics and dynamics of a parallel manipulator with a new architecture, *Robotica* **18**, 535–543 (2000).
12. O. Didrit, M. Petitot and E. Walter, Guaranteed solution of direct kinematic problems for general configurations of parallel manipulators, *IEEE Trans. Robotics Automat.* (April), 259–266 (1998).
13. B. Dasgupta and T. S. Mruthyunjaya, *The Stewart Platform Manipulator: A Review*. Elsevier Science, Amsterdam (2000).
14. V. Hayward and R. Kurtz, Modeling of a parallel wrist mechanism with actuator redundancy, *Int. J. Lab. Robotics Automat.* **4**, 69–76 (1992).
15. V. Hayward, Design of a hydraulic robot shoulder based on a combinatorial mechanism, in: *Experimental Robotics III: The 3rd Int. Symposium*, Lecture Notes in Control and Information Sciences, pp. 297–310. Springer, Berlin (1994).
16. V. Hayward, Borrowing some design ideas from biological manipulators to design an artificial one, in: *Robots and Biological System*, NATO Series, pp. 135–148. Springer, Berlin (1993).
17. H. Sadjadian and H. D. Taghirad, Numerical methods for computing the forward kinematics of a redundant parallel manipulator, in: *Proc. IEEE Conf. on Mechatronics and Robotics*, Aachen, pp. 557–562 (2004).
18. C. Gosselin and J. Angeles, Singularity analysis of closed-loop kinematic chains, *IEEE Trans. Robotics Automat.* **6**, 281–290 (1990).
19. G. Liu, Y. Lou and Z. Li, Singularities of parallel manipulators: a geometric treatment, *IEEE Trans. Robotics Automat.* **19**, 579–594 (2003).
20. B. S. El-Khasawneh and P. M. Ferreira, Computation of stiffness and stiffness bounds for parallel link manipulators, *Int. J. Machine Tools Manufact.* **00**, 321–342 (1999).
21. C. Gosselin, Stiffness mapping for parallel manipulators, *IEEE Trans. Robotics Automat.* **6**, 377–382 (1990).

22. D. R. Kerr, Analysis, properties, and design of a Stewart platform transducer, *ASME J. Mech. Transmiss. Automat. Des.* **111**, 25–28 (1989).
23. L. W. Tsai, *Robot Analysis: The Mechanics of Serial and Parallel Manipulators*. Wiley, New York (1999).

ABOUT THE AUTHORS

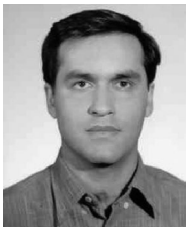

Hooman Sadjadian received his BS degree in Electrical Engineering from Tehran University, Tehran, Iran, in 1995 and his ME in Electrical Engineering from Iran University of Science and Technology, Tehran, Iran, in 1999. He is currently a PhD student with the Electrical Engineering Department, K. N. Toosi University of Technology, Tehran, Iran. His research interests are the dynamics and control of parallel manipulators.

Hamid D. Taghirad received his BS degree in Mechanical Engineering from Sharif University of Technology, Tehran, Iran, in 1989, and his ME in Mechanical Engineering in 1993 and his PhD in Electrical Engineering in 1997, both from McGill University, Montreal, Canada. He is currently an Associate Professor with the Electrical Engineering Department, Control Group, and the Director of the Advanced Robotics and Automated System, ARAS Research Center at K. N. Toosi University of Technology, Tehran, Iran. He became a member of the IEEE in 1995. His publications include two books, and more than 90 papers in international journals and conference proceedings. His research interests are robust and non-linear control applied on robotic systems.